

Evaluation of Optimized Multisectioned Acoustic Liners

Kenneth J. Baumeister*

NASA Lewis Research Center, Cleveland, Ohio

A critical examination is presented of the use of optimized axially segmented acoustic liners to increase the attenuation of a liner. New calculations show that segmenting is most efficient at high frequencies with relatively long duct lengths where the attenuation is low for both uniform and segmented liners. Statistical considerations indicate little advantage in using optimized liners with more than two segments, while the bandwidth of an optimized two-segment liner is shown to be nearly equal to that of a uniform liner. Multielement liner calculations show a large degradation in performance, due to changes in assumed input model structure. Finally, in order to substantiate previous and future analytical results, in-house (finite difference) and contractor (mode matching) programs are used to generate theoretical attenuations for a number of liner configurations for liners in a rectangular duct with no mean flow. Overall, the use of optimized multisectioned liners (sometimes called phased liners) fails to offer sufficient advantage over a uniform liner to warrant their use, except in low-frequency, single-mode application.

Nomenclature

c_0^*	= speed of sound
ΔdB	= sound attenuation
F	= function
f^*	= frequency
H^*	= channel height
i	= $\sqrt{-1}$
L^*	= length of duct
M	= Mach number
m	= transverse mode number
p	= dimensionless Fourier coefficient of pressure, $p(x,y), p^*/p_A$
p_A	= amplitude of pressure fluctuation or $\rho_0^* c_0^{*2}$
x	= dimensionless axial coordinate, x^*/H^*
x^*	= axial coordinate
y	= dimensionless transverse coordinate, y^*/H^*
y^*	= transverse coordinate
δ	= fractional impedance variation
ζ	= specific acoustic impedance
η	= dimensionless frequency $f^* H^*/c_0^*$ or $\omega^* H^*/2\pi c_0^*$
η_{eff}	= $\eta H^*/L^*$
θ	= specific acoustic resistance
ρ_0^*	= density
χ	= specific acoustic reactance
ω^*	= circular frequency

Subscripts

I	= interface
s	= segmented (see Figs. 6, 9, and 13)
u	= uniform (see Figs. 6, 9, and 13)

Superscript

*	= dimensional quantity
---	------------------------

Introduction

TO eliminate the need for heavy, expensive, and otherwise undesirable splitter rings, and also to reduce the required length of wall treatment (cowl length), recent research has

been concerned with increasing the attenuation of wall treatment in a fixed length of liner. For fixed source frequency and modal content, one approach to increasing the attenuation of a given liner is to subdivide the liner into several different segments that are jointly optimized to maximize the noise attenuation over that of a uniform optimized liner.

The NASA Lewis Research Center has conducted both in-house¹ and contract studies^{2,3} concerning the optimization of axially segmented ducts. Herein, a critical examination is presented of the use of optimized axially segmented acoustic liners (sometimes called phased liners) to increase the attenuation of a liner. In performing this examination, first, in order to substantiate previous and future analytical results, in-house (finite difference) and contractor (mode matching) programs are used to generate theoretical attenuations for a number of liner configurations in a rectangular duct with no mean flow. Next, new calculations are presented for the noise attenuation of optimized segmented ducts. These calculations consider the effects of sound frequency, duct length, number of segments, uncertainty in wall impedance, and variations in modal input of the sound. In addition, the bandwidth of optimized segmented liners is also investigated. Before beginning the analysis, a brief review of the literature is now given.

Wilkinson (Ref. 4, p. 13) first attempted to improve the attenuation of a uniform optimized duct by breaking the liner into two sections and optimizing each section individually. His optimization routine gave impedance values for the two sections which were nearly identical to that of a uniform liner (Ref. 4, Table 1); consequently, only a 6% enhancement in attenuation over the uniform liner was obtained. Lansing and Zorumski,⁵ however, showed that a multisectioned (three-section) liner could give a 60% increase in attenuation for a liner configuration which was not actually optimized. The details of the theory presented in Ref. 5 are presented by Zorumski in Ref. 6.

Baumeister¹ and Quinn,⁷ using a finite-difference approach, both showed that optimized two- and three-segment liners would greatly increase the attenuation over a uniform liner of the same length. In Ref. 6, Zorumski speculated that a reflection process was responsible for the behavior of multisectioned ducts. In contrast to Zorumski's hypothesis, Baumeister¹ showed by detailed pressure plots that the mechanism of added transmission loss for an initially plane wave in a multisectioned duct seems to be a conditioning of the sound in the first section, which makes it susceptible to

Presented as Paper 79-0182 at the AIAA 17th Aerospace Sciences Meeting, New Orleans, La., Jan. 15-17, 1979; submitted Jan. 22, 1979; revision received April 30, 1979. This paper is declared a work of the U.S. Government and therefore is in the public domain. Reprints of this article may be ordered from AIAA Special Publications, 1290 Avenue of the Americas, New York, N.Y. 10019. Order by Article No. at top of page. Member price \$2.00 each, nonmember, \$3.00 each. Remittance must accompany order.

Index category: Aeroacoustics.

*Aerospace Engineer.

absorption in the following sections. The first section conditions the acoustic modes such that the acoustic power is brought close to the walls (Ref. 1, Fig. 12). This modal redistribution (or modal scattering) mechanism was later verified by Sawdy et al. (Ref. 2, p. 16).

The first parametric study of the effect of frequency on segmented liner attenuation was attempted by Quinn (Ref. 7, Fig. 1). Unfortunately, an error in computer programming gave larger attenuation at the lower frequencies than can be expected, as shown by Motsinger et al. (Ref. 3, Fig. 75). Quinn (Ref. 7, Fig. 2) also indicated that the bandwidth of a multisectioned liner is considerably greater than that of a uniform liner for fixed impedance. Since impedance is a strong function of frequency, the initial work of Quinn will be extended herein to include the effects of sound frequency on liner impedance in a bandwidth study.

In Ref. 2 and the additional papers derived from this work,⁸⁻¹⁰ Sawdy et al. analyzed and measured the properties of optimal multisectioned ducts using an interface mode-matching method. They showed that a three-segment liner can be designed to be less sensitive to modal input. They, simultaneously with Ref. 3, presented experimental tests of the optimized multielement concept in rectangular ducts. In Refs. 2 and 10, the data (centerline pressure measurements) are shown to verify the modal conditioning mechanism (Ref. 10, Fig. 21); they also show that segmented linings can be used to provide more attenuation than optimum single-element configuration.

In Ref. 3 and its additional conference papers,^{11,12} Motsinger et al., using a mode-matching technique shown in both their analytical and experimental programs that changes in source modal content affect the performance of a two-segment suppressor. Also, their error analysis showed large sensitivity in predicted attenuation to small wall impedance variations from the optimum.

Motsinger et al. (Ref. 3, Fig. 75) showed that the increase in attenuation of a two-element liner over a uniform liner occurs in a confined dimensionless frequency range of η from 1 to 5 with a peak in attenuation near $\eta=1.5$. These and other symbols are defined in the list of symbols. Lester and Posey showed similar results (Refs. 13 and 14, Fig. 9). They also showed that the optimum based on modal theory agrees with the geometric acoustic theories at high frequencies.

Koch¹⁵ showed that the Wiener-Hopf technique can also be applied to segmented liners. He investigated the effect of various liner properties, such as backing depth, resistance, etc., on the attenuation of segmented liners; however, he did not optimize the liners for maximum performance. Unruh¹⁶ has performed optimal calculations for the special case of hard-soft-hard ducts. He found a lining length tuning effect which allows for a more efficient lining design than can be predicted by infinite duct theory. Wyerman and Reethof¹⁷ have investigated the problem of higher-order acoustic modes in multisectioned ducts. The results of their study suggest that better liner performance might be obtained by using segmented duct configurations made up by a combination of several different liner materials.

Method of Analysis

The calculations of the propagation of sound in a liner will be performed herein by a numerical finite-difference technique. Figure 1a shows a typical finite-difference grid network used in Ref. 18 to study the propagation of sound in a two-dimensional duct in the absence of flow. Assuming that the pressure is a simple harmonic function of time ($e^{i\omega t}$) and that no source exists in the medium, the linearized gasdynamic equations (Ref. 19, p. 5) of continuity, momentum, and energy reduce to the dimensionless Helmholtz equation:

$$\frac{\delta^2 p}{\delta x^2} + \frac{\delta^2 p}{\delta y^2} + (2\pi\eta)^2 p = 0 \quad (1)$$

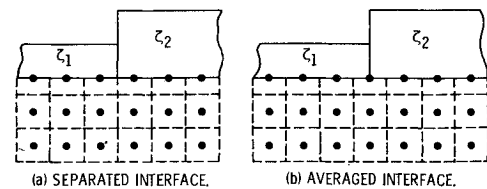


Fig. 1 Numerical treatment of wall impedance discontinuity.

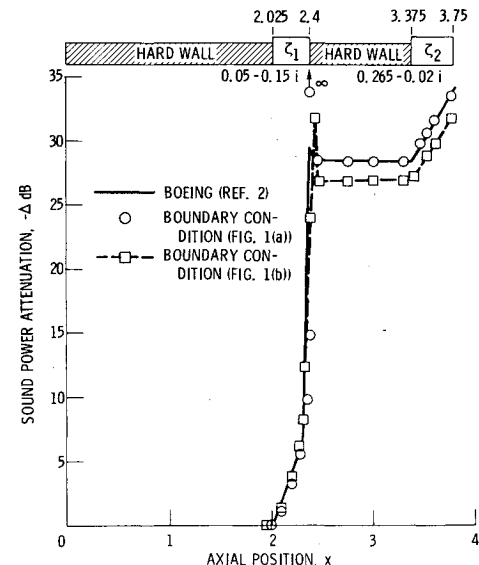


Fig. 2 Comparison of sound power attenuation for mode-matching and finite-difference solution at optimum impedance for $\eta=0.25$, $M=0$.

which governs the propagation of sound in the duct.

To solve Eq. (1) using finite-difference techniques, the derivatives in Eq. (1) are expressed in terms of pressure at each grid point. For the boundary conditions, an entrance pressure profile, an exit impedance, and a specific acoustic wall impedance ζ are required. The specific acoustic wall impedance ζ is composed of a resistive part θ and a reactive component χ , such that

$$\zeta = \theta + i\chi \quad (2)$$

Between two liner segments, the grid points can straddle the interface, as in Fig. 1a, or ride on it, as in Fig. 1b. In the latter case, Fig. 1b, the impedance associated with the interface grid point, can be shown to be

$$\zeta_I = 2 / (1/\zeta_1 + 1/\zeta_2) \quad (3)$$

using the procedure of Ref. 18, Appendix D.

The collection of the various difference equations at each grid point in the duct and along the boundary form a set of simultaneous equations which are solved to determine the pressure at each grid point. From these pressures, the acoustic particle velocities, sound intensity, and noise attenuation can be found. The complete details of the finite-difference technique can be found in Ref. 18.

Configuration Calculations

The attenuation of a few sample two-element liner configurations are now calculated using the finite-difference techniques just described and then compared with NASA's contractor calculations using the mode-matching techniques of Refs. 2 and 3. The calculations will be compared and tabulated for possible use in checking the validity of existing and future multielement analytical routines. The sample

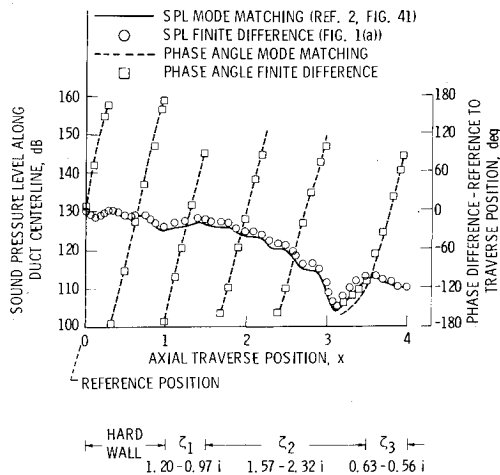


Fig. 3 Comparison of mode-matching and finite-difference predicted axial distribution of centerline pressure magnitude and phase for liner with three soft wall segments and input modal distribution $p = 1 + (0.35 - 0.15j) \cos(2\pi y)$ where $y=0$ is centerline, $M=0$, $\eta = 1.52$.

calculations apply to an initially plane wave input for a straight rectangular duct infinite in length without mean flow.

Figure 2 compares the sound power attenuation for the mode-matching and finite-difference calculations for η equal to 0.25 and L^*/H^* of 3.75. The impedances shown at the top of Fig. 2 represent optimum impedances (associated with maximum sound attenuation) for this symmetric configuration. As seen in Fig. 2, the local sound power attenuation values are in close agreement. However, both the mode-matching and finite-difference techniques show a spike at the $x=2.4$ interface. The spike results from the mathematical singularity which exists at the optimum. The total attenuation for the liner is approximately 34 dB.

The off-optimum behavior of the theories was also examined by slightly changing the reactance of ζ_l in Fig. 2 from $0.15i$ to $0.1i$. In this case (not shown), both theories are in still better agreement with a total attenuation of about 21 dB. Also, the spike no longer appears at the $x=2.4$ interface for either interface condition shown in Fig. 1.

Figure 3 represents another comparison between the mode-matching and finite-difference methods for a four-segment duct containing three soft wall segments. In this case, the SPL pressure levels and phase of both techniques show good agreement.

It should be noted that the optimal liner resistance of the first section of a three-segment liner (Fig. 3) is much larger than that of a two-segment liner (Fig. 2). Reference 2 (p. 20) found this to be the general case, although one exception was noted. As will be shown later in this paper, the resistance of the first liner segment will be a strong function of liner length.

So far, the agreement between mode-matching and finite-difference theory is excellent, which leads to a degree of confidence in the accuracy of the predicted results. However, based on some sample problems of Ref. 2, some discrepancies still exist between the various theories. Table 1 again shows good agreement between the various programs for off-optimum results (Table 1a); however, near the optimum (Table 1b), the various theories yield significantly different results for $\eta = 1.6$, although the $\eta = 0.25$ results are in good agreement, as also shown in Fig. 2. Only one propagating acoustic mode exists in the latter case. Because the attenuation associated with the optimum point is often very peaked, perhaps the more precise analytical mode-matching technique may resolve the peak. In this case, the finite-difference theory yields conservative results. At the present time, however, no exact explanation exists to account for these differences. Further work is required.

We have just discussed, in relation to Fig. 2, how a single 0.05 impedance perturbation can significantly change the attenuation at the optimum. From a practical point of view, it may be necessary to design a multielement liner based on impedance values slightly perturbed from the optimum impedance. This could eliminate the problem just described. The effect of uncertainty in liner impedance will be discussed in more detail later in this report.

Plane Wave Parametric Studies

This section will be concerned with determining how the optimum attenuation and impedance are related to sound frequency, duct length, and number of liner segments. First, the liner is subdivided into several different but fixed-length liner segments. Next, to obtain higher attenuations than are possible with a uniform liner, the liner segments are optimized

Table 1 Computer program prediction results

a) Far from optimum						
Liner segments	Frequency, η	Impedance, ζ	Length	Attenuation, dB		
				Boeing	GE	Lewis
2	1.6	1.0-1.4 i	0.526	-15.5	-15.3	-16.1
		1.58-1.34 i	2.474			
3	1.6	0.35-0.85 i	0.5	-9.97	-9.8	-10.42
		0.87-1.77 i	2.0			
		0.35-0.85 i	0.5			
4	0.25	∞	2.025	-21.4	—	-20.62
		0.05-0.1 i	0.375			
		∞	0.975			
		0.265 + 0.02 i	0.375			
b) Near optimum						
2	1.6	0.048-1.7 i	0.841	-40.8	-39.7	-30.25
		1.44-0.84 i	2.159			
3	1.6	0.917-0.981 i	0.470	-50.4	-42.5	-32.2
		1.579-2.205 i	1.959			
		0.601-0.497 i	0.571			
4	0.25	∞	2.025	-34.1	-36.56	-34.71
		0.05-0.15 i	0.375			
		∞	0.975			
		0.265 + 0.02 i	0.375			

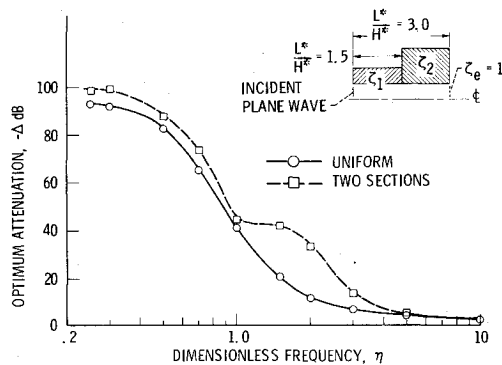


Fig. 4 Optimum predicted sound power attenuation in rectangular duct with uniform and two-segment treatment for L^*/H^* equal to 3, $M=0$.

jointly to maximize the noise attenuation. In the optimization process, the starting point was the optimized uniform impedance. The first liner segment then was optimized while holding the remaining segments at the uniform value. Next, holding the first segment at its new value, the iteration process was continued on the remaining segments. The process was repeated for the whole liner until the change in duct attenuation was less than 5%. This optimum does not necessarily represent the global optimum, since the optimum is sensitive to the assumed starting impedance.²

In all the examples to follow, the input pressure source will be a plane wave and, as in Ref. 18, the exit impedance of the duct will be assumed to be $\rho_0^* c_0^*$.

Effect of Frequency η

Figure 4 shows the optimum attenuation as a function of η for a two-segment liner which has a geometric configuration identical to that considered by Motsinger (Ref. 3, Fig. 75), except in this case the Mach number is zero instead of the 0.3 value of Ref. 3. The results here are similar to those reported by Motsinger et al.³ Using these limited examples, one is lead to conclude that segmented treatment is most effective at low η values. However, exactly the opposite is the case, as will now be discussed.

Effective Frequency, η_{eff}

Baumeister (Ref. 20, p. 22) transformed the wave equation into a form which did not depend explicitly on frequency. From consideration of the system parameters, he suggested correlating the duct attenuation as a function of an effective frequency which incorporates treatment length into the definition of frequency

$$\eta_{\text{eff}} = \eta H^*/L^* \quad (4)$$

Therefore, Figs. 5 and 6 which follow, show a treatment length effect. As shown in Fig. 5, the optimum attenuation for various frequencies and duct length can be correlated in terms of η_{eff} .

In Fig. 6, the ratio of optimum attenuation duct ΔdB_s to an optimized uniform duct ΔdB_u is plotted again as a function of η_{eff} for various η . As seen in Fig. 6, the attenuation increases with η with the peak occurring with $\eta H^*/L^*$ about 1. It should be noted, however, that for the high values of η , where the greatest benefit of segmented treatment over uniform liners occurs, both have quite low attenuations, as seen in Fig. 5.

Figures 7 and 8 show the optimum impedance for $\eta=1$. As in Ref. 2, the optimum specific acoustic resistance θ was constrained to be at least 0.04. For large values of L^*/H^* , as shown in Figs. 7 and 8, the resistance and reactance of the two segments approach the uniform value.

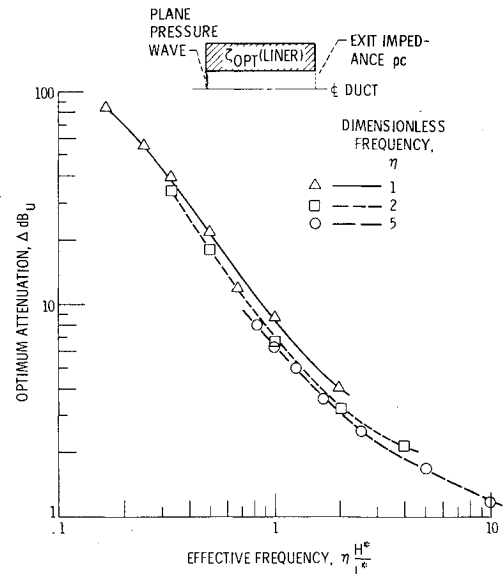


Fig. 5 Relation between optimum attenuation and effective frequency for uniform liner, $M=0$.

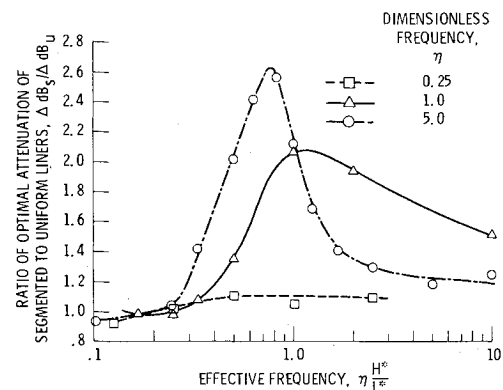


Fig. 6 Increase in optimized liner attenuation resulting from segmented liners ($M=0$, two segments of equal length).

Three-Segment Liners

The attenuation of a liner can be enhanced by further subdivisions. As seen in Fig. 9, increasing the number of optimized segments from two to three yields an 80% increase in attenuation of the three-segment liner over the two-segment liner. The resistance and reactance associated with the three-segment liner is shown in Figs. 10 and 11. As seen in Fig. 10, as with the two-segment liners, the initial resistance is low for small values of L^*/H^* and increases for increasing L^*/H^* . From practical considerations, however, a three-segment liner may not give significantly more attenuation than a two-segment liner, as will be shown later.

Unequal Liner Lengths

Equal length segments have been assumed for the multielement liners. The optimum attenuation of a two-segment liner with unequal lengths has been calculated by Motsinger et al. (Ref. 3, Fig. 78) for a dimensionless frequency $\eta=1.535$. If the ratio of length of the first to second liner is between 1 and 2, the optimum attenuation is nearly constant and equal to the value obtained for equal segments. If the ratio of the length of the first to second liner approaches zero, then the attenuation will approach the optimum value for a uniform liner. Therefore, the limited parametric study of Ref. 3 indicates that equal liner segments will yield the maximum attenuation for two-segment liners.

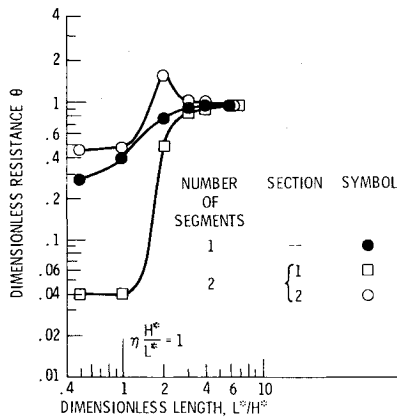


Fig. 7 Optimum resistance for uniform and two-section liners ($L_1=L_2$) for $\eta=1.0$, $M=0$.

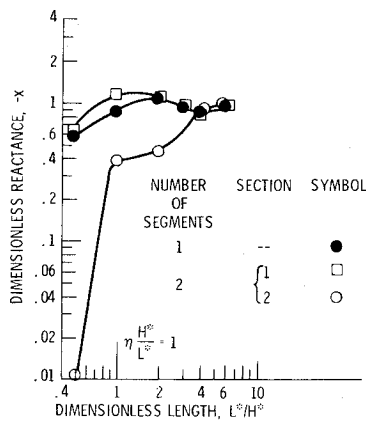


Fig. 8 Optimum reactance for uniform and two-section liners ($L_1=L_2$) for $\eta=1.0$, $M=0$.

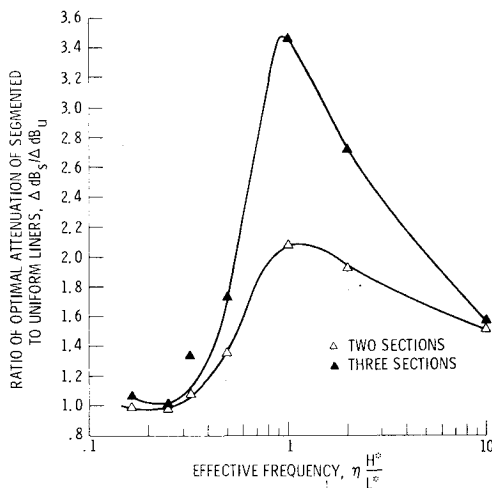


Fig. 9 Increase in optimized liner attenuation resulting from segmented liners ($M=0$, two- and three-segment liners, equal liner segments, dimensionless frequency $\eta=1$, and plane wave input).

Uncertainty Consideration

The actual impedance of a liner will deviate from the optimum value because of fabrication tolerances, as well as from the uncertainty in the impedance correlations. To estimate the uncertainty in the attenuation of a liner, the ΔdB is assumed to be a function of the impedance values. That is,

$$\Delta \text{dB} = F(\theta_1, \chi_1, \theta_2, \chi_2, \dots, \theta_n, \chi_n) \quad (5)$$

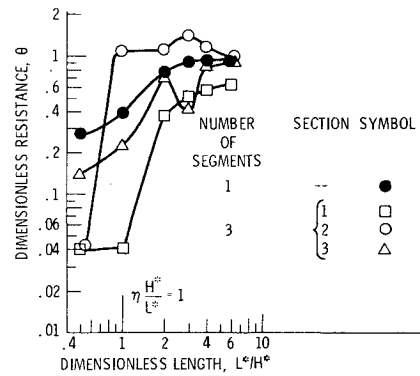


Fig. 10 Optimum resistance for uniform and three-section liners ($L_1=L_2=L_3$) for $\eta=1.0$, $M=0$.

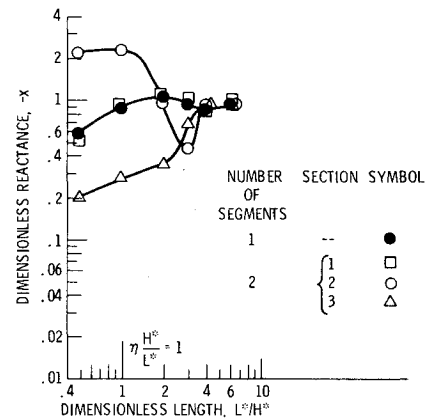


Fig. 11 Optimum reactance for uniform and three-section liners ($L_1=L_2=L_3$) for $\eta=1$, $M=0$.

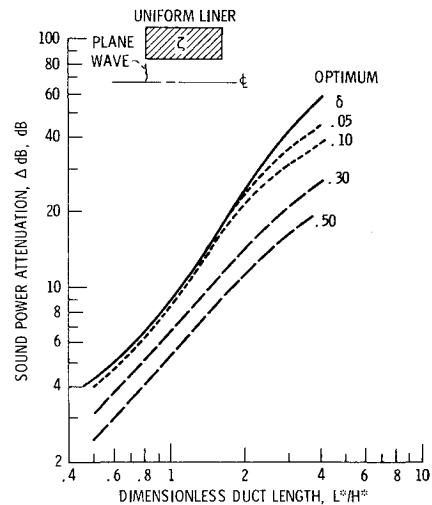


Fig. 12 Effect of impedance variations from optimum and axial length on the sound power attenuation of a uniform liner at a dimensionless frequency $\eta=1.0$ and $M=0$.

Since the optimum represents a discontinuity in attenuation, the standard formula for calculating the uncertainty of a function of several variables (Ref. 21, p. 22) cannot be used.

To give a measure of the effect of uncertainty in attenuation due to liner impedance variation, it was assumed that all the impedance values simultaneously changed a given amount. This gives a "maximum possible" attenuation loss for the assumed variation in impedance.

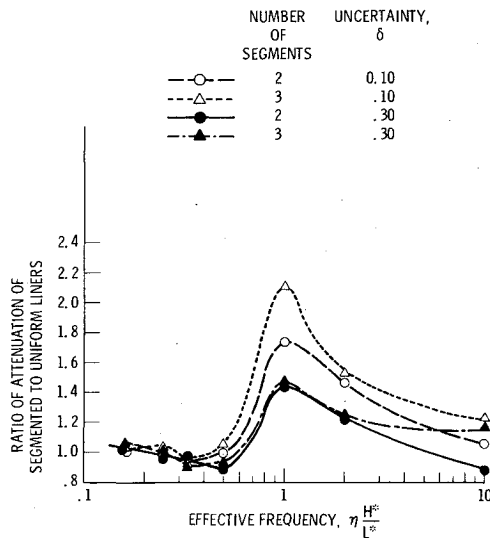


Fig. 13 Effect of uncertainties in liner impedance on optimal attenuation of segmented liners ($\eta = 1$, equal length segments, $M = 0$).

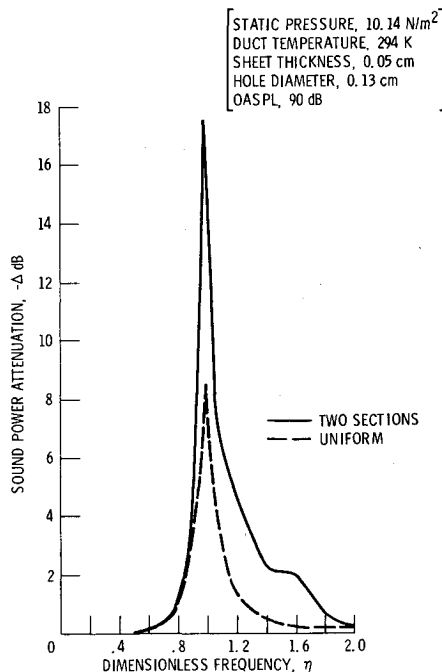


Fig. 14 Bandwidth comparisons of optimized uniform and two-segment liners for $\eta_{opt} = 1.0$, $L^*/H^* = 1.0$, $H^* = 30.48$ cm, and $M = 0$.

Let the parameter δ represent the fractional change in impedance due to uncertainty. Furthermore, let

$$\begin{aligned} \theta &= \theta_{opt} + \delta & \theta_{opt} < 1 \\ &= \theta_{opt} + \delta_{opt} \theta_{opt} & \theta_{opt} \geq 1 \end{aligned} \quad (6)$$

$$\begin{aligned} \chi &= \chi_{opt} + \delta & |\chi_{opt}| < 1 \\ &= \chi_{opt} + \delta |\chi_{opt}| & |\chi_{opt}| \geq 1 \end{aligned} \quad (7)$$

A range of values of δ from 0.05 to 0.5 will be considered in the analysis. From the graphical results, estimates of the attenuation change due to δ can be conveniently made.

Figure 12 shows the expected decrease in the sound power attenuation of a uniform liner. Similar results occur for a two-

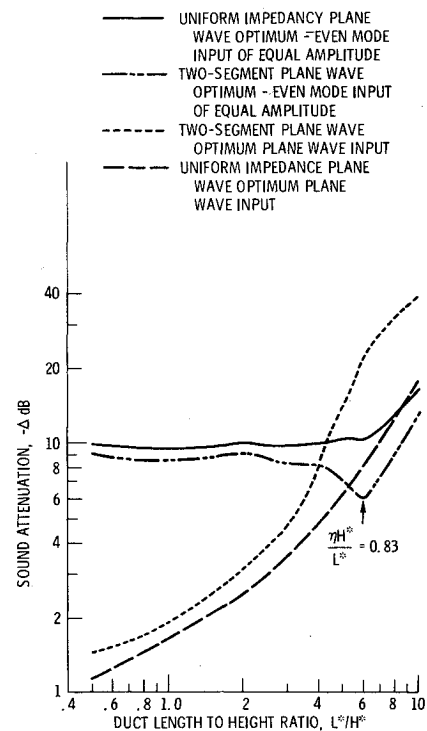


Fig. 15 Sensitivity of optimum design to change in input modal structure at $\eta = 5$ and $M = 0$.

segment liner for the same geometry and frequency; however, the loss of attenuation for a given δ is greater for the two-segment liner than the uniform liner.

Figure 13 summarizes the results for both the two- and three-section liners in which the ratio of the attenuation of the multisectioned to uniform liner is shown. The same percentage impedance errors are included in each type of liner. As seen in Fig. 13, if δ is on the order of 0.3, which is a practical value, then the three-segment liner offers little advantage over the two-segment liner. Also observe that in the vicinity of $\eta H^*/L^* = 0.6$, the uniform liner has greater sound-absorbing capability than the multisectioned liners.

Bandwidth

In this section, the bandwidth of the two-segment liner will be evaluated near the point of maximum enhanced attenuation ($\eta H^*/L^* = 1$). The values of optimum impedance for $\eta = 1$ can be found in Figs. 7 and 8. Once the required value of acoustic liner impedance is specified, the mathematical model relating impedance to the geometric parameters can be used to calculate the liner open area ratio and backing depth. The basic equations of the impedance model which are semiempirical were reported by Groeneweg in Ref. 22, and will not be repeated here.

Minner and Rice (Ref. 23, p. 24) have reformulated these equations into a form which allows a simple direct calculation for the open area ratio and backing depth. Once the open area and backing depth are known, the resistance and reactance can be calculated directly from the formulas in Ref. 22.

Figure 14 shows the bandwidth curves for uniform and two-segment liners optimized at $\eta = 1$. The two-segment liner curve, shown in Fig. 14, shows some increased attenuation at the higher frequencies with a very modest increase in bandwidth.

Two additional bandwidth calculations were performed and will now be discussed without the use of figures. For a liner optimized at $\eta = 0.25$, subdividing the liner into two sections gave almost identical bandwidth compared to the uniform liner. For a liner optimized at $\eta = 5$, the uniform and

two-segment liner bandwidth curves are similar in form to those shown in Fig. 14, except the hump to the right of the peak does not appear.

At the present time, the bandwidth characteristics of optimized two-element liners do not appear to show any significant improvement over uniform liners. These examples, however, do not represent a large range of system parameters.

Sensitivity to Input Modal Structure

In a hard wall rectangular duct, the nondimensional acoustic pressure can be expressed as (Ref. 24, Appendix B)

$$p = \sum_{n=1}^{\infty} A_n \cos n\pi y e^{-i\pi\sqrt{(2\eta)^2 - n^2}x} \quad (8)$$

where the transverse mode ($\cos n\pi y$) will propagate unattenuated if

$$n < 2\eta \quad (9)$$

The previous parametric studies were for plane wave input. However, at higher input frequencies η , as seen in Eq. (9), the input could be other than a plane wave, because the number of propagation modes becomes large with increased η . Therefore, some sample calculations were performed to test the effect of source modal structure on a uniform and two-segment plane wave optimized liner.

The modal structure investigated considered all propagating even modes with constant amplitude and equal phase at $\eta = 5$. The choice of only even modes was made for best resolution in the finite-difference analysis, since only one-half of the duct needed to be considered. This modal structure was used as the pressure source in both uniform and two-segment liners that had been designed for plane wave input.

As seen in Fig. 15, changing from a plane wave input to a multimodal input in the uniform single-element duct shows a large improvement in attenuation at low L^*/H^* . At high L^*/H^* , the attenuation is nearly the same as for the plane pressure wave. Therefore, a single-segment liner design based on a plane wave input does not experience any degradation in performance over the entire L^*/H^* range. The single-element optimal liner design for this multimode source will, of course, increase the attenuation above that shown in Fig. 15.

On the other hand, the plane wave optimized two-segment liner experiences a large degradation in performance at $L^*/H^* = 6(\eta H^*/L^* = 0.83)$. Recall from Fig. 6, the maximum enhancement of the multielement liner was at this point. Also, for the nonplane wave, the uniform liner has higher performance than the two-segment liner. Clearly, multielement liners appear to be much more sensitive to modal input. This was also shown indirectly in Ref. 2 (p. 22, Table 4) in which the optimum impedance for a multielement liner was found to be a strong function of the modal content of the source.

In addition, both the single-element and the two-segment liners were reoptimized for this new multimodal source. In this case, the two-element liner attenuation, as expected, exceeded that of the single-element liner. However, the ratio of attenuation of the two-element to the single-element liner at the peak attenuation was 1.73. This is a large decrease from the 2.6 value shown in Fig. 6 for the plane wave source.

The multimode source chosen here has its peak pressure at the walls. The decrease in maximum enhanced attenuation from 2.6 to 1.73 might indicate that if the noise energy is already concentrated near the walls, the advantage of the optimized two-element liner will not be as great. Recall that the function of the first element in the two-segment liner was to concentrate the acoustic energy near the wall.

In a practical liner used for fairly high frequency, the modal input is seldom known and changes as the source conditions change, for example, as the engine speed changes.

Thus it is questionable whether a multisectioned liner which is very sensitive to modal input would provide much advantage in a real suppressor environment. However, for very low frequencies and small duct dimensions where a plane wave is the only allowable mode, the multisectioned liner may provide greatly increased attenuation.

Conclusions

Axially segmented liners are shown to theoretically increase the attenuation over a uniform liner of the same length for $\eta H^*/L^*$ values ranging between 0.4-5 for a plane wave excitation with a maximum attenuation enhancement occurring with $\eta H^*/L^*$ about equal to 1. The segmenting is most efficient at high frequencies with relatively long duct lengths. However, for the high values of η where the greatest benefit of segmented treatment over uniform liners occurs, both have quite low attenuations. Statistical considerations indicate little advantage in using optimized liners with more than two segments. Bandwidth studies of optimized two-segment liners also show little advantage over a uniform optimized liner. Finally, multielement liners show a large degradation in performance due to changes in the assumed input modal structure. Overall, the use of optimized axially segmented liners (sometimes called phased liners) fails to offer sufficient advantage over a uniform liner to warrant their use except in low-frequency, single-mode application.

References

1. Baumeister, K. J., "Wave Envelope Analysis of Sound Propagation in Ducts with Variable Axial Impedance," *AIAA Progress in Astronautics and Aeronautics—Aeroacoustics: Fan Noise and Control; Duct Acoustics; Rotor Noise*, edited by I. R. Schwartz, New York, 1976, pp. 451-474.
2. Sawdy, D. T., Beckemeyer, R. J., and Patterson, J. D., "Analytical and Experimental Studies of an Optimum Multisegment Phased Liner Noise Suppression Concept," Boeing Company, D3-9812-1, May 1976; NASA CR-134960.
3. Motsinger, R. E., Kraft, R. E., Zwick, J. W., Vukelich, S. I., Minner, G. L., and Baumeister, K. J., "Optimization of Suppression for Two-Element Treatment Liners for Turbomachinery Exhaust Ducts," General Electric Co., R76AEG256, April 1976; NASA CR-134997.
4. Wilkinson, J. P. D., "The Calculation of Optimal Linings for Jet Engine Inlet Ducts, Part II," NASA CR-1832, Aug. 1971.
5. Lansing, D. L. and Zorumski, W. E., "Effects of Wall Admittance Changes on Duct Transmission and Radiation of Sound," *Journal of Sound and Vibration*, Vol. 27, March 1973, pp. 85-100.
6. Zorumski, W. E., "Acoustic Theory of Axisymmetric Multisectioned Ducts," NASA TR R-419, 1974.
7. Quinn, D. W., "Attenuation of Sound Associated with a Plane Wave in a Multisectioned Duct," *AIAA Progress in Astronautics and Aeronautics, Aeroacoustics: Fan Noise and Control; Duct Acoustics; Rotor Noise*, edited by I. R. Schwartz, Vol. 44, New York, 1976, pp. 331-345.
8. Beckemeyer, R. J. and Sawdy, D. T., "Optimization of Duct Acoustic Liners of Finite Length," Paper No. H1, *Proceedings of the 89th Meeting of the Acoustical Society of America*, Austin, Texas, April 1975.
9. Sawdy, D. T., Beckemeyer, R. J., and Patterson, J. D., "Optimum Segmented Acoustic Liners for Flow Ducts," Paper D6, *Proceedings of the 90th Meeting of the Acoustical Society of America*, San Francisco, Calif., Nov. 1975.
10. Patterson, J. D., Sawdy, D. T., and Beckemeyer, R. J., "Experimental-Analytical Correlation of Optimum Duct Acoustic Liner Performance," ASME Paper 76-GT-126, March 1976.
11. Motsinger, R. E., Kraft, R. E., and Zwick, J. W., "Design of Optimum Acoustic Treatment for Rectangular Duct with Flow," ASME Paper 76-GT-113, March 1976.
12. Kraft, R. E. and Motsinger, R. E., "Practical Consideration for the Design of Two-Element Duct Liner Noise Suppressors," *AIAA Paper 76-517*, July 1976.
13. Lester, H. C. and Posey, J. W., "Duct Liner Optimization for Turbomachinery Noise Sources," NASA TM X-72789, 1975.
14. Lester, H. C. and Posey, J. W., "Optimal One-Section and Two-Section Circular Sound-Absorbing Duct Liners for Plane-Wave and Monopole Sources Without Flow," NASA TN D-8348, 1976.

¹⁵Koch, W., "Attenuation of Sound in Multi-Element Acoustically Lined Rectangular Duct in the Absence of Mean Flow," *Journal of Sound and Vibration*, Vol. 52, June 1977, pp. 459-496.

¹⁶Unruh, J. F., "Finite Length Tuning for Low Frequency Lining Design," *Journal of Sound and Vibration*, Vol. 45, March 1976, pp. 5-14.

¹⁷Wyerman, B. R. and Reethof, G., "The Propagation of Plane Waves and Higher-Order Acoustic Modes in Multisectioned Ducts," Pennsylvania State University, University Park, Pa., Sept. 1975; NASA CR-143438.

¹⁸Baumeister, K. J., "Finite-Difference Theory for Sound Propagation in a Lined Duct with Uniform Flow Using the Wave Envelope Concept," NASA TP-1001, Aug. 1977.

¹⁹Goldstein, M. E., *Aeroacoustics*, McGraw Hill Book Co., Inc., New York, 1976.

²⁰Baumeister, K. J., "Analysis of Sound Propagation in Ducts Using the Wave Envelope Concept," NASA TN D-7719, 1974.

²¹Wolberg, J. R., *Prediction Analysis*, D. Van Nostrand, Princeton, N.J., 1967.

²²Groeneweg, J. F., "Current Understanding of Helmholtz Resonator Arrays as Duct Boundary Conditions," *Basic Aerodynamic Noise Research*, I. R. Schwartz, ed., NASA SP-207, 1969, pp. 357-368.

²³Minner, G. L. and Rice, E. J., "Computer Method for Design of Acoustic Liners for Turbofan Engines," NASA TM X-3317, 1976.

²⁴Baumeister, K. J., "Numerical Spatial Marching Techniques for Estimating Duct Attenuation and Source Pressure Profiles," Paper H7, *Proceedings of the Meeting of the Acoustical Society of America*, Providence, R. I., May 1978; also NASA TM X-78857.

From the AIAA Progress in Astronautics and Aeronautics Series . . .

RADIATION ENERGY CONVERSION IN SPACE—v. 61

Edited by Kenneth W. Billman, NASA Ames Research Center, Moffett Field, California

The principal theme of this volume is the analysis of potential methods for the effective utilization of solar energy for the generation and transmission of large amounts of power from satellite power stations down to Earth for terrestrial purposes. During the past decade, NASA has been sponsoring a wide variety of studies aimed at this goal, some directed at the physics of solar energy conversion, some directed at the engineering problems involved, and some directed at the economic values and side effects relative to other possible solutions to the much-discussed problems of energy supply on Earth. This volume constitutes a progress report on these and other studies of SPS (space power satellite systems), but more than that the volume contains a number of important papers that go beyond the concept of using the obvious stream of visible solar energy available in space. There are other radiations, particle streams, for example, whose energies can be trapped and converted by special laser systems. The book contains scientific analyses of the feasibility of using such energy sources for useful power generation. In addition, there are papers addressed to the problems of developing smaller amounts of power from such radiation sources, by novel means, for use on spacecraft themselves.

Physicists interested in the basic processes of the interaction of space radiations and matter in various forms, engineers concerned with solutions to the terrestrial energy supply dilemma, spacecraft specialists involved in satellite power systems, and economists and environmentalists concerned with energy will find in this volume many stimulating concepts deserving of careful study.

690 pp., 6 × 9, illus., \$24.00 Mem. \$45.00 List

TO ORDER WRITE: Publications Dept., AIAA, 1290 Avenue of the Americas, New York, N. Y. 10019